Fatigue Behavior in Nickel-Based Superalloys: A Literature Review

L. Garimella, P.K. Liaw, and D.L. Klarstrom

Authors' Note: Inconel, Incoloy, and Nicalon are registered trademarks.

In this literature review, the present understanding regarding the effects of microstructure, loading conditions, and environments on the fatigue behavior of nickel-based superalloys is reviewed.

INTRODUCTION

Superalloys are alloys developed for elevated-temperature service; the term was first used shortly after World War II to describe a group of alloys developed for use in turbosuperchargers and aircraft-turbine engines that required high-temperature performance. In addition to good high-temperature strength, superalloys also exhibit oxidation and corrosion resistance.

Superalloys usually consist of various formulations made from elements such as nickel, cobalt, iron, and chromium as well as lesser amounts of W, Mo, Ta, Nb, Ti, and Al. Many types of alloys come under the broad coverage of superalloys, including iron-based alloys containing chromium and nickel, complex iron-nickel-cobalt compositions, carbide-strengthened cobalt-based alloys, solid-solution strengthened cobalt-based alloys, and precipitation- or dispersion-strengthened nickel-based alloys. Superalloys are used both in wrought and cast form.

The high-temperature applications of superalloys are extensive, including components for aircrafts, chemical-plant equipment, and petrochemical equipment. Superalloys are used as disks, bolts, shafts, cases, blades, vanes, burner cans, afterburners, and thrust reversers in aircraft and industrial gas turbines; stock gas reheaters in steam-turbine power plants; turbochargers, exhaust valves, hot plugs, precombustion cups, and valve-seat inserts in reciprocating engines; hot-work tools and dies and cast dies in metal processing; prosthetic devices and dentistry; aerodynamically heated skins and rocket-engine parts in space vehicles; trays, conveyors, and fixtures in heat-treating equipment; and control-rod drive mechanisms, valve stems, springs, and ducts in nuclear power plants.

Nickel-based superalloys are the most widely used of all the classes of superalloys. (Descriptions of some of the superalloys beyond nickel-based alloys are readily available in the literature.[1-25]) They have a complex composition and good high-temperature properties, and their use extends to the highest homologous temperature of any common alloy system.[1]

Fatigue properties in nickel-based alloys are affected by different parameters relating to microstructural and testing conditions.

A great deal of attention is currently being given to the low-cycle fatigue performance of superalloys, particularly in the field of turbine-engine designs, where there is every indication that it is likely to become the deciding factor in the selection of an alloy. Besides providing fundamental information relating to the performance of individual alloys, low-cycle fatigue data may be applied to predict the life of engineering components when subjected to a similar straining cycle as that simulated in a laboratory. Fatigue properties in nickel-based alloys are affected by different parameters relating to microstructural and testing conditions.

FATIGUE BEHAVIOR

For several decades, fatigue has been known as one of the major causes of failure in engineering structures. Several parameters have now been identified as playing significant roles in affecting the growth of defects.[26-57] These are intrinsic parameters like alloying, heat treatment, microstructure, and elasto-plastic behavior; the mechanical factors such as the crack geometry, load amplitude, and stress load ratio* and the physico-chemical parameters, including the nature, composition, and temperature of the environment surrounding the crack tip.

Most materials for engineering applications are subjected to fluctuating stresses; this accounts for a large number of failures. These failures are due to fatigue and must be distinguished from static failures. Most failures are due to a combination of steady-state and cyclic stresses. The contribution of each of these stresses would depend on a host of parameters, which would include the relative stress levels for each and the temperature of operation. Superalloys must constantly combat the result of the superposition of these stresses at elevated temperatures. Hence, failure in most cases is neither pure fatigue nor pure creep. The study of these mechanisms is important since it gives an insight into the contribution of each.

Fatigue testing encompasses all mechanical testing in which fluctuating stresses are considered. Hence, a wide range of different conditions are involved. A high proportion of fatigue tests are conducted with specific engineering applications in view. This makes it difficult to compare the results of different alloys. The available data are sometimes of limited applicability, and the comparison of properties is not straightforward.

Fatigue can be classified in many ways based on different parameters. Based on the number of cycles for failure, it can be

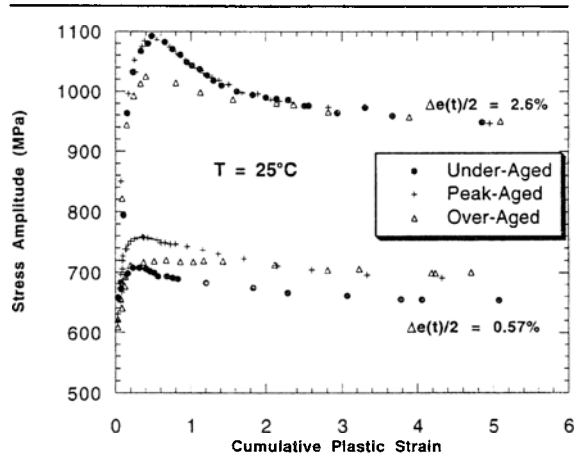

Figure 1. Cyclic response curves for the underaged, peak-aged, and overaged materials as a function of cumulative plastic strain tested at $\Delta e(t)/2 = 0.60$ and 2.60%.[30]

* Stress ratio, otherwise called load ratio or R-ratio, is defined as $\sigma_{min}/\sigma_{max}$, where σ_{min} and σ_{max} are the minimum and maximum stresses, respectively.

broadly classified into two regimes: the high-cycle fatigue and the low-cycle fatigue. The early works were represented as S-N curves that showed the change in the cycles to failure (N) for a variation in the stress amplitude (S) on a semilogarithmic scale.

After establishing the dependence of crack-growth-rates (da/dN) on the stress-intensity-factor range (ΔK), fatigue results are also depicted by plotting these values on a log-log scale. Typically these plots conform to the Paris equation

$$da/dN = C(\Delta K)^n \qquad (1)$$

where C and n are the material constants. Such plots were first critically scrutinized by Paris and Erdogan.[27] Eventually, the curve is divided into three regions: the near-threshold crack-growth region, the stable crack-growth region or the Paris region, and the unstable crack-growth region. In the near-threshold region, there is a threshold stress-intensity-factor range (ΔK_{th}) below which the crack would not grow or would grow at an extremely slow rate (approximately 10^{-10} m/cyc). Fatigue-crack-growth theories primarily address the derivation of the Paris equation.

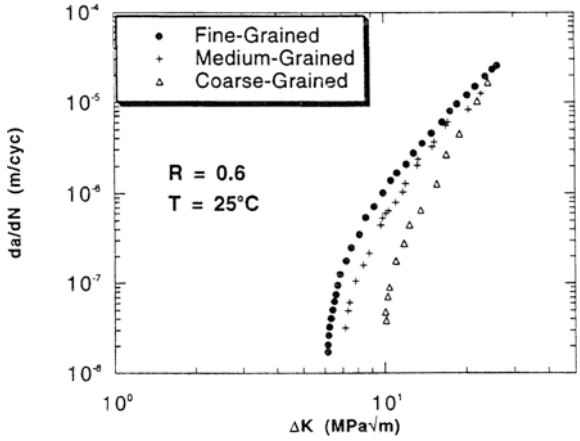

Figure 2. The effect of grain size on fatigue crack-growth rates for AP-1.[33]

MICROSTRUCTURAL PARAMETERS OF FATIGUE

Microstructure

Microstructure plays an important role in determining the fatigue and fracture properties of nickel-based superalloys. Aging accompanied by the precipitation of γ′ precipitates leads to enhanced fatigue properties. A study done by Bartosiewicz et al.[28] on Incoloy 825 showed the effect of aging on fatigue properties. It was found that the crack-growth rates were lower for materials that had been aged to peak hardness as compared to specimens that were underaged and specimens that were as-received. Higher ΔK_{th} and lower crack-growth rates in the threshold region for the underaged and aged samples can be explained on the basis of the crack closure[29] phenomenon. The underaged and aged samples exhibit crack closure, which reduces the effective stress intensity factor range. Hence, the driving force for the crack propagation decreases, which results in lower crack-growth rates relative to the as-received samples.

A similar study was conducted by Singh et al.[30] on Nimonic alloy PE16, where the low-cycle fatigue properties were studied by varying the aging time. Figure 1 displays the variation of stress amplitude, $\Delta\sigma/2$, against the cumulative plastic strain, $\Sigma\Delta\varepsilon_p$, for small- and large-strain amplitudes. The maximum stress generally increases with increasing the γ′ particle size up to the peak-aged condition and decreases thereafter in the overaged condition. The cumulative plastic strain at which the maximum stress is achieved increases

COMPOSITION AND MICROSTRUCTURE

Some of the main alloying elements used in nickel-based superalloys include Cr, Al, Ti, Nb, Fe, Co, Mo, W, Ta, V, B, Zr, and C.

The addition of chromium is done primarily to increase corrosion and oxidation resistance. Optimum corrosion properties are expected with the addition of 15–30 wt.% chromium, which also forms chromium carbides when carbon is present, leading to precipitation hardening.

Most nickel-based alloys derive their strength by the precipitation of γ′ precipitates. The elements responsible for this strengthening are aluminum, titanium, and niobium. The γ′ precipitates are $Ni_3(Ti,Al)$. When niobium is present in excess of 4 wt.%, it forms a separate hardening phase, Ni_3Nb, which is designated as the γ″ phase. When present in lesser amounts, niobium substitutes for aluminum and titanium in the γ′ precipitates. Both titanium and niobium also form carbides, which give additional strengthening effects. Aluminum also helps in the high-temperature oxidation resistance by forming an impervious oxide on the alloy surface.

The addition of iron is done to make the alloy cost effective. There is a limitation in the inordinate increase of iron, as this leads to a decrease in the oxidation resistance. Iron also leads to the formation of a sigma phase that has a deleterious effect on the properties. The addition of cobalt enhances the high-temperature strength, and reduces the solubility of aluminum and titanium in the nickel-chromium matrix. Cobalt has been shown to increase the workability of nickel-based superalloys, especially those with high contents of aluminum and titanium.[3]

Solid-solution strengthening is provided at high temperatures by the addition of molybdenum, tungsten, and tantalum. They also dissolve in γ′ precipitates and enhance strengthening properties. Molybdenum, tungsten, and tantalum also form complex carbides with each other and with iron and chromium, leading to increased strength properties.

Boron and zirconium are added to improve creep strength and ductility. They segregate to the grain boundaries and slow down the agglomeration of grain-boundary carbides.[4] Ni, Co, Fe, and Cr belong to the matrix class and form the matrix of the particular superalloy. When not forming the matrix, the addition of these elements, along with W, Mo, and V, gives solid-solution strengthening. Ta, Ti, Al, and Nb are added for precipitation hardening. C, B, and Zr belong to the grain-boundary subclass. Some of the elements (e.g., Cr, Mo, W, V, Nb, Ta, and Ti) also form carbides. Elements such as chromium and aluminum form oxides and, hence, belong to the oxide-scale subclass.

The microstructure of nickel-based alloys typically comprises a face-centered cubic (fcc) austenitic matrix called the γ phase. It shows finely dispersed precipitates that are the γ′ phase. The morphology and distribution of the precipitates can change with time. The secondary phases consist primarily of carbides of varying compositions, morphology, and distribution.

The different structural features present in a nickel-based alloy are the alloy matrix (γ), gamma prime (γ′), grain boundary γ′, γ″ precipitates, carbides, and topologically close-packed (tcp) phases. The alloy matrix forms a continuous matrix in nickel-based alloys, which is a nickel-based austenitic phase that has other alloying elements like chromium, cobalt, molybdenum, and tungsten in solid solution. Gamma prime are mainly precipitates of $Ni_3(Ti,Al)$ in the alloy matrix. They are coherent precipitates, and their volume fraction is kept high to enhance the structural properties. The grain boundary γ′ is precipitated along the grain boundary with special heat treatments to enhance the rupture properties, while γ″ precipitates are Ni_3Nb precipitates having a DO_{22} crystal structure; they are precipitated to obtain enhanced strength. Carbides are formed when carbon combines with the reactive elements in the alloy matrix. Some carbides are precipitated with undesirable morphologies that deteriorate the alloy properties. Topologically close-packed phases are formed under certain conditions in the microstructure. They have been classified as μ, Laves, and σ phases. They have a deleterious effect on the strength and rupture properties.

Strengthening Mechanisms

The high-strength and creep-rupture properties of nickel-based alloys result from a number of strengthening mechanisms. The strength of the alloy depends on the grains and the grain boundary. At less than $0.6T_m$ (T_m is the melting point of the alloy), the strength is predominantly determined by the deformation of the grains. The main strengthening mechanisms that come into play are solid-solution strengthening and precipitate hardening. At temperatures above $0.6T_m$, the alloys are affected by relative grain movement and rotation, coupled with grain-boundary sliding. The formation of carbides at the grain boundaries contributes to the strength at these temperatures.

The rules for solid solutions have been laid down by Hume-Rothery's principles. The strengthening is enhanced when there is a wide range in solid solution coupled with a large dissimilarity in the atomic sizes. Hardening is related to the atomic diameter oversize, as measured by the lattice expansion.[8]

The increase in strength is attributed to the decrease of the stacking-fault energy, making it difficult to cross slip. This behavior would be particularly useful at high temperatures, where diffusion and dislocation cross slip are important in determining the strength. A study was undertaken by Pelloux and Grant[8] to explain the effect of various additions on the strength of nickel-based alloys. Their results show the change in the yield stress of the material for every 0.001 nm change in the lattice parameter caused by the addition of alloying elements.

This strengthening mechanism relies primarily on the precipitation of γ′ phase, which is typically an A_3B compound. It is precipitated in high-nickel matrices.

with increasing particle size. This study revealed that the cyclic-stress response curve is determined by the operating dislocation-precipitate interaction mechanism. When precipitate shearing is the dominant mechanism (underaged and peak-aged conditions), the initial hardening is generally followed by a period of softening. For the overaged condition where both Orowan looping and precipitate shearing are operating, the extent of hardening and softening is relatively small. At low strain amplitudes, the number of cycles to achieve the maximum stress in underaged and peak-aged materials is attained within a narrow range of cycles. The number of cycles for the maximum stress continuously decreases with an increase in the strain amplitude for the overaged state.

Grain Size

Grain size has also been shown to influence fatigue properties. In a study conducted by Denda et al.[31] on Inconel 718, it was observed that the coarse-grained material exhibits shorter low-cycle fatigue life than the fine-grained material, despite its slower crack-growth rates. Similar results have been observed by Krueger et al.[32]

A similar study to understand the effect of grain size on fatigue properties was done by Kim and Knott.[33] The grain size had a large influence on the near-threshold fatigue crack-growth rate and ΔK_{th} (Figure 2). Crack-growth rates were reduced and threshold values increased as the grain size increased. Increasing the grain size results in a decrease of yield stress and an increase in the roughness of the fracture surface, and, consequently, the roughness-induced crack closure. The higher roughness-induced crack closure in the coarse-grained material decreases the effective stress-intensity-factor range ($\Delta K_{eff.} = K_{max.} - K_{closure}$, where $K_{max.}$ is the maximum stress intensity factor and $K_{closure}$ is the stress intensity corresponding to the crack closure), which results in slower crack-propagation rates. Similarly, at low R-ratios, crack-propagation rates were reduced during faceted crack-growth by increasing the grain size.[34]

The study conducted by Bartosiewicz et al.[28] on Incoloy 825 revealed similar results. Here, it was found that ΔK_{th} tends to increase with an increase in grain diameter; this is observed due to a greater extent of roughness-induced crack closure at higher grain sizes.

γ'' Morphology and Distribution

The morphology and volume fraction of γ' and/or γ'' precipitates affect the crack-growth behavior and the low-cycle fatigue life.[32] A study conducted on Inconel 718 showed that finer precipitates result in a slower long-crack growth rate and longer low-cycle fatigue life in many cases.[32,35] The short-crack-growth behavior is not significantly affected by changes occuring in the precipitate morphology. It has been estimated that the finer precipitates can result in an extension of the short-crack propagation regime.

Floreen and Kane[36] speculated that the homogenization of slip and, consequently, the minimization of localized stress concentrations at the grain boundaries through changes in the precipitate morphology are a way in which the overaging heat treatment could increase resistance to high-temperature crack growth. Smith and Michel[37] suggested that the improvement in the crack-growth resistance produced by a modified heat treatment is likely to be a result of the alteration of mechanisms of dislocation interactions with γ' particles and grain boundaries. The works of Smith and Michel,[37] Pedron and Pineau,[38] and Zheng and Ghonem[39] have shown that by coarsening the γ'' precipitate particles, the mechanism of dislocation motion will be altered from a mechanism involving the shearing of precipitate par-

These precipitates were first observed as spherical particles, then as cubes, and later in many other geometrical forms. Its shape was later related to the matrix-lattice mismatch. The change in morphology with lattice mismatch has been studied by Hagel and Beattie.[9] The γ' particles have been precipitated in the form of spherical, trigonal, elongated, or cubical morphologies. There exist many other variations in size and shape.

The γ' precipitates are based on the formula $Ni_3(Ti,Al)$ with variable amounts of titanium and aluminum; the nickel in this compound can be replaced to some extent by Co, Mo, Cr, and Fe. The important aspects of this phase are that it is finely precipitated, and it is coherent with the matrix. This provides for a low surface energy, which makes these precipitates stable at high temperatures for long times. Since the γ' precipitates are ductile, it does not cause embrittlement when precipitated at the grain boundaries. The other precipitate that forms in these alloys is the η phase. It has a body-centered-tetragonal (bct) structure and forms as platelets. It also can have a variable composition.

The strengthening obtained by the precipitation of these phases is due to the generation of dislocations and the impedance of dislocation movement. There are several factors that influence the effectiveness of γ' in impeding the dislocation movement. For a dislocation to move past a precipitate, it either has to cut through it, or loop around it by a mechanism known as Orowan looping.[12] The interparticle distance determines which of the above mechanisms is in operation. The minimum radius of curvature to which a matrix dislocation can be bent is given by

$$\rho_{min} = T/\tau b \qquad (A)$$

where T is the line tension of a dislocation of Burger's vector b, and τ is the applied stress. Dislocation loops are formed when the interparticle distance is greater than $2\rho_{min}$. When the interparticle distance is less, the dislocations pass by cutting through the particles.

An analysis of dislocation interactions with a coherent precipitate in a fcc lattice was done by Gleiter and Hornbogen.[14] When a dislocation enters an ordered phase, it creates an antiphase domain boundary (APB) on the slip plane that, being a high-energy area, strengthens the alloy.[15] Gleiter and Hornbogen derived an expression that related the increase in yield stress, Δτ, caused by the presence of γ' precipitates to precipitate parameters.

$$\Delta\tau \propto f^{\frac{1}{3}} r_0^{\frac{1}{2}} \Gamma^{\frac{2}{3}} \qquad (B)$$

where f is the volume fraction of γ', r_0 is the γ' particle radius, and Γ is the APB radius.

At a given temperature, the volume fraction of γ' is directly proportional to the amount of alloying additions added for hardening. This was confirmed by Gibbons and Hopkins[16] in a Ni-20Cr base. The relationship between the volume fraction of the precipitate and the stress-rupture properties at different temperatures was determined by Decker.[17] His result showed the change in 100 hours of the stress-rupture life with the change in γ' vol.% for different temperatures as valid for a range of nickel-based superalloys.

It has been ascertained that the relationship between the γ' particle size and the alloy strength is determined by the way in which the dislocations bypass the particles. The volume fraction of γ' in most commercial nickel alloys is such that when γ' is below a critical size, particle cutting occurs. In this regime, the strength is proportional to $r_0^{1/2}$. During service when the particles coalesce, dislocation looping can take place. As the particle size increases, the strengthening mechanism changes from Orowan looping to particle cutting.

Most commercial nickel-based alloys have carbon contents upwards of 0.02 wt.%. The carbon present in the alloys forms different metal carbides, both inside the grains and at the grain boundaries. The effect of carbides inside the grain is minimal due to the presence of the evenly precipitated γ' phase. The intergranular carbides play an important role in the strengthening process.

Carbides are harder and more brittle than the alloy matrix, and hence, the nature in which they are precipitated at the grain boundary is important. A continuous film of carbide along the grain boundary is deleterious, as it can form a continuous fracture path. It would also prevent grain-boundary sliding during creep, which would lead to excessive stress buildup and premature fracture. An optimum amount and distribution of carbides along the grain boundary would prevent excessive grain-boundary sliding and the growth of voids during high-temperature deformation. This leads to enhanced creep-rupture properties.

Several types of carbides can be formed in the alloy. Monocarbides of the type MC are formed during the melting and are very stable. Here, M can be substituted by Ti, Ta, Nb, or W. More complex carbides, such as $M_{23}C_6$, M_7C_3, or M_6C, are also formed. The carbides may be present as blocky particles, degenerated particles at the grain boundary, cellular particles, or fine or coarse particles inside the grain or at the grain boundary.

Commercial nickel-based alloys require a careful control of the composition to prevent the precipitation of undesirable TCP phases. The commonly found phases in nickel-based alloys are σ, μ, and Laves phases. They are composed of closed-packed layers of atoms forming in kagome nets, aligned with the octahedral planes of the fcc γ matrix.[21] These phases appear as thin plates, often nucleating at the grain boundaries. The common precipitates mainly have a plate-like morphology.

The strength loss is due to the brittle plate-like morphology, which forms an excellent site for crack initiation and propagation. This feature causes low-temperature embrittlement. Since they contain a high amount of metal content taken from the alloy matrix γ, it leads to weakening. It has been shown that high-temperature rupture fracture occurs along the σ phase, rather than at the grain boundaries.[22]

ticles to that of bypassing by the Orowan process.

TEST PARAMETERS

Stress Ratio

Stress ratio has an important bearing on the fatigue crack-growth properties. Bartosiewicz et al.[28] have shown that as the load ratio increases for Incoloy 825, the fatigue crack-growth rate in the threshold region increases. The change in rates is dependent on the microstructure. It was observed that the effect of the load ratio on crack growth is much smaller in the Paris region than in the threshold region.

Vosikovsky[40] showed that the value of ΔK_{th} decreases with an increase in the stress ratio. He proposed an empirical relationship

$$\Delta K_{th} = \Delta K_{tho} (1-bR) \qquad (2)$$

where ΔK_{tho} is the value of the threshold stress-intensity-factor range at R-ratio = 0, and b is a material constant. Barsom[41] also observed a linear relationship between ΔK_{th} and R-ratio. Klensil and Lukas[42] observed a nonlinear power law relationship between ΔK_{th} and the stress ratio.

Kim and Knott[33] showed the R dependency of fatigue crack-growth rates for alloy AP-1 (Figure 3). At low crack propagation rates where faceted growth occurs, it was observed that grain coarseness led to high stress-intensity-range values at low load ratios (< 0.5). The decrease in ΔK_{th} with increasing load ratio was explained by the crack closure phenomenon. At higher R-ratios (≥ 0.5), the $K_{min.}$ is higher than $K_{closure}$, where $K_{min.}$ is the minimum stress-intensity factor. Hence, the total stress-intensity-factor range effectively contributes to crack propagation at higher R-ratios. At lower R-ratios, the values of $\Delta K_{eff.}$ are reduced by the $K_{closure}$. Therefore, lower ΔK_{th} values are observed at higher R-ratios.

Liaw and Logsdon[43] showed the effects of R-ratio on the fatigue crack-growth properties of Inconel 706 for different specimen orientations. Figure 4 shows the influence of stress ratio at 24°C and –268.8°C on the near-threshold fatigue crack-growth behavior in the CR orientation (where the loading direction is along the circumferential direction of the disk-shaped test material, and the crack is propagating along the radial direction). At 24°C in the CR orientation, increasing the R-ratio from 0 to 0.8 significantly increased the rates of crack propagation. Correspondingly, the value of ΔK_{th} at R = 0.1 was 1.9 times greater than that at R = 0.8. Furthermore, decreasing the ΔK level increased the influence of R-ratio on crack-growth rates, which is characteristic of the near-threshold crack propagation behavior. At –268.8°C, the crack-growth rates were relatively insensitive to R-ratio. Similar results were obtained for the RC orientation (where the loading direction is along the radial direction of the disk-shaped test material, and the crack propagates along the circumferential direction). At lower R-ratios at 24°C, the higher crack closure levels, attributed to oxide and/or roughness-induced crack closure, decrease the effective stress-intensity-factor ranges, yielding lower near-threshold crack-growth rates and higher ΔK_{th} values. The oxide levels for Inconel 706 were fairly thin, therefore, the extent of oxide-induced crack closure at threshold levels was minimal at both temperatures. At –268.8°C, roughness-induced crack closure is minimal due to smooth fracture surfaces, which results in little influence of R-ratio on ΔK_{th}.

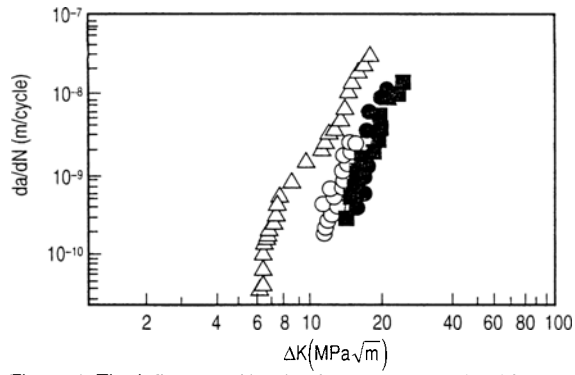

Figure 4. The influence of load ratio on near-threshold fatigue crack-growth behavior at –268.8°C and 24°C in CR orientation. —T = 24°C, R-Ratio = 0.1, specimen designation = 706-R5 (R5); —T = 24°C, R-Ratio = 0.8, specimen designation = 706-I2 (I28); ●—T = –268.8°C, R-Ratio = 0.1, specimen designation = 706-R4 (R4); ■—T = –268.8°C, R-Ratio = 0.8, specimen designation = 706-R4 (R48).[43]

Frequency

Fatigue properties are influenced by the frequency of the load or strain cycles. Fatigue crack-growth behavior is determined by the loading pattern and the characteristic response of the alloying materials. Generally, transgranular failure is observed when cycled at high frequencies (around 10 Hz). At low frequencies (around 0.05 Hz), the crack-growth mode becomes highly rate sensitive, with intergranular failure predominant. Hsu[44] showed this trend for Inconel 617, which maintains the predominantly transgranular mode even as the loading frequencies are reduced. However, they fail intergranularly when creep or steady loading are imposed. The effect of frequency on fatigue properties is illustrated in Figure 5. The figure shows that the crack-growth rate increases as the frequency decreases from 5 Hz to 0.016 Hz. This occurs because at lower frequencies the material experiences a longer time at higher stresses in an oxidizing environment, which gives higher crack-growth rates.

Experimental studies have been carried out by several authors[45–49] investigating the effect of loading frequency on fatigue crack-growth mechanisms in alloy 718 in both air and vacuum environments at elevated temperatures. Ghonem et al.[50,51] have shown that the slip-line density increases proportionally with loading frequency. The crack-growth mode at higher frequencies (10–15 Hz) is mostly transgranular. As the test frequency decreases (0.1–0.01 Hz), the crack-tip damage becomes a combination of oxidation and cycle-dependent components.

Testing Environment

The effect of environment on the time dependence of high-temperature crack growth has been well documented in literature. Smith et al.[52] have demonstrated that environmental degradation is a result of oxygen penetration at the crack tip. Oxidation mechanisms can be broadly grouped into short- and long-range oxygen diffusion processes. In short-range diffusion,[53–56] oxides are formed at the crack tip, which results in high stresses that cause rupture at grain-boundary intersections and, consequently, accelerated intergranular crack-growth rates. In long-range diffusion, oxygen diffuses along slip planes and grain boundaries and reacts to form embrittlement agents.

Andrieu et al.[57] observed a change in the fracture mode in their study on the crack-tip oxidation mechanisms of

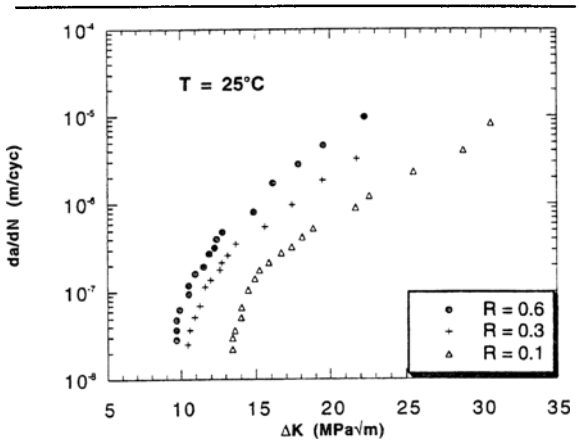

Figure 3. The effect of stress ratio on fatigue crack-growth rate tests for a Nimonic AP-1 alloy with coarse grains.[33]

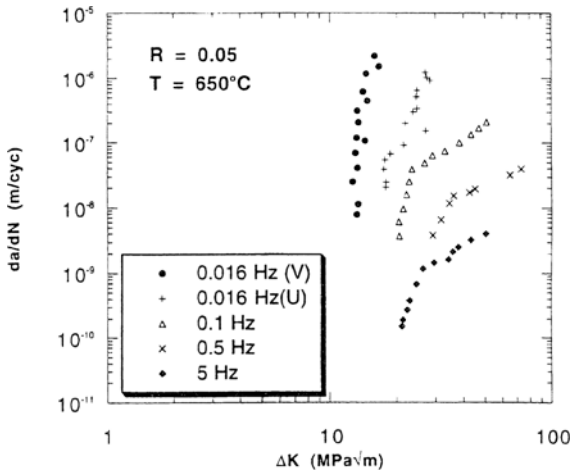

Figure 5. Crack-growth rate per cycle versus stress intensity factor range for five fatigue tests at varying cycle frequencies for Inconel 617.[44]

Inconel 718 from completely intergranular to completely transgranular when the testing environment changed from air to vacuum. These results indicate the total domination of the environment on the crack-growth properties. The effect of testing environment on the crack-growth behavior was conducted by Ghonem and Zheng.[50] It was observed that the crack-growth rates were considerably higher for the material tested in air as compared to the material tested in vacuum. A short-range diffusion mechanism with the formation of spinel-oxide type followed at the metal-oxide interface by a protective chromia layer, which increases the crack propagation rates.

CONCLUSIONS

Based on our literature survey, relatively little work has focused on the high-cycle fatigue crack initiation and small fatigue crack propagation behavior of superalloys. With the rapid and advanced development of crack-detection capabilities such as atomic force microscopy and scanning tunneling microscopy, it is important to investigate the mechanistic aspect of fatigue crack initiation behavior. Particularly, the influence of high test frequency in the range of 500–5,000 Hz on fatigue crack initiation behavior needs to be emphasized, since a majority of aircraft and land-based engine components made of superalloys are in operation at high frequencies.

References

1. C.T. Sims and W.C. Hagel, *The Superalloys* (New York, John Wiley & Sons, 1972).
2. A.M. Filippi, NASA TN D-4955 (1968).
3. J. Heslop, *Proc. Journees Int. des Applications du Cobalt* (1964), p. 209
4. R.F. Decker and J.W. Freeman, *Trans. AIME*, 218 (1960), p. 277.
5. C.T. Sims, ASME tech. pub. 70-GT-24 (1970).
6. E.F. Bradley, *Superalloys: A Technical Guide* (Metals Park, OH: ASM, 1988).
7. R.F. Decker, "Strengthening Mechanisms in Nickel-Base Superalloys," *Climax Molybdenum Company Symposium* (Zurich: Climax Molybdenum Co., 1969).
8. R.M.N. Pelloux and N.J. Grant, *Trans. AIME*, 218 (1960), p. 232.
9. W.C. Hagel and H.J. Beattie, *Iron and Steel Inst. Spec. Rep.* 64 (1971), p. 98.
10. W.B. Kent, "Mechanical Properties and Structural Characteristics of NASA IIb" (Paper presented at the AIME Annual Meeting, Cleveland, Ohio, 1970).
11. J.R. Mihalisin, personal communication.
12. E. Orowan, *Symposium on Internal Stresses in Metals and Alloys* (London: IOM, 1948), p. 451.
13. *The Nimonic Alloys*, eds. W. Betteridge and J. Heslop (New York: Crane, Rusack and Company, 1974).
14. H. Glieter and E. Hornbogen, *Phys. Stat. Sol.*, 12 (1965), p. 235.
15. R.O. Williams, *Acta. Met.*, 5 (1957), p. 241.
16. T.B. Gibbons and B.E. Hopkins, *Met. Sci. J.*, 5 (1971), p. 233.
17. R.F. Decker, *Steel Strengthening Mechanisms* (Zurich: Climax Molybdenum Company, 1969), p. 147.
18. W.I. Mitchell, *Z. Metall.*, 57 (1966), p. 586.
19. R.W. Smashey, personal communication.
20. C.T. Sims, *J. Met.*, 18 (10) (1966).
21. H.J. Beattie, Jr., and W.C. Hagel, *Trans AIME*, 233 (1965), p. 277.
22. E.W. Ross, "Recent Research on IN-100," (Paper presented at the AIME Annual Meeting, Dallas, TX, 1963).
23. H.J. Murphy, C.T. Sims, and G.R. Heckman, *Trans. AIME*, 236 (1967), p.1961.
24. L.R. Woodyatt, C.T. Sims, and H.J. Beattie, Jr., *Trans. AIME*, 236 (1966), p. 519.
25. H.J. Beattie, Jr., and W.C. Hagel, *Trans. AIME*, 221 (1961), p. 28; *Trans. AIME*, 215 (1959), p. 973.
26. G. Henaff, K. Marchal, and J. Petit, *Acta Met.*, 43 (8) (1995), p. 2931.
27. P.C. Paris and F. Erdogan, *Trans. ASME-J. Basic Eng.*, 85 (1963), p. 528.
28. L. Bartosiewicz et al., *J. Mater. Engr. and Performance*, 1 (1992), p. 67.
29. W. Elber, *Eng. Fract. Mech.*, 21 (1970), p. 323.
30. V. Singh et al., *Met. Trans. A*, 22A (1991), p. 499.
31. T. Denda, P.L. Bretz, and J.K. Tien, *Met. Trans A*, 23A (1992), p. 519.
32. D.D. Krueger, S.D. Antolovich, and R.H. Van Strom, *Met. Trans. A*, 18A (1987), p. 1431.
33. S. Kim and J.F. Knott, *Fracture & Strength '90 Key Engrg. Mater.*, 51 (1991), p. 209.
34. J.E. King, *Met. Sci.*, 16 (1982), p. 345.
35. E.A. Schwarzkopf, Ph.D. thesis, Columbia University (1989).
36. S. Floreen and R.H. Kane, *Fatigue Eng. Mater. Struct.*, 2 (1980), p. 401.
37. H.H. Smith and D.J. Michel, *Ductility and Toughness Considerations in Elevated Temperature Service*, MPC-8, ed. G.V. Smith (New York: ASME, 1978), p. 269–277.
38. J.P. Pedron and A. Pineau, *Mater Sci. Eng.*, 56 (1982), p. 143.
39. D. Zheng and H. Ghonem, *Met. Trans. A*, 23A (1992), p. 3169.
40. O. Vosikovsky, *Eng. Fract. Mech.*, II (1979), p. 595.
41. J.M. Barsom, *WRC Bull.*, 194 (1974), p. 33.
42. M. Klensil and P. Lukas, *Mater. Sci. Eng.*, 9 (1983), p. 231.
43. P.K. Liaw and W.A. Logsdon, *Acta. Met.*, 36 (7) (1988), p. 1731.
44. S.S. Hsu, *Scripta. Met.*, 25 (1991), p. 1143.
45. L.A. James, *J. Eng. Mater. Tech.*, 95 (1973), p. 254.
46. M. Clavel and A. Pineau, *Met. Trans. A*, 95 (1978), p. 471.
47. S. Floreen and R.H. Kane, *Fatigue Eng. Mater. Struct.*, 2 (1980), p. 401.
48. T. Weerasooriya and S. Venkataraman, *Effect of Load and Thermal Histories on Mechanical Behavior of Materials*, eds. P.K. Liaw and T. Nicholas (Warrendale, PA: TMS, 1987).
49. T. Weerasooriya, *Fracture Mechanics: 19th Symp.*, ASTM STP 969, ed. T.A. Cruse (Philadelphia, PA: ASTM, 1988).
50. H. Ghonem and D. Zheng, *Mater. Sci. Eng.*, 150A (1992), p. 151.
51. H. Ghonem, T. Nicholas, and A. Pineau, "High Temperature Effects" (Paper presented at the ASME Winter Annual Meeting, Atlanta, GA, 1991).
52. H.H. Smith, P. Shahinian and M.R. Achter, *Trans. Am. Inst. Min. Eng.*, 245 (1969), p.947.
53. R.H. Bricknell and D.A. Woodford, *Met Trans. A*, 12 (1981), p. 425.
54. C.J. McMahon and L.F. Coffin, *Met. Trans.*, 1 (1970), p. 3443.
55. L.F. Coffin, ASTM STP 520 (1973), p. 5.
56. C.J. McMahon, Jr., *Mater. Sci. Eng.*, 13 (1974), p. 295.
57. E. Andrieu et al., *Mater. Sci. Eng.*, 154 (1992), p. 21.

ABOUT THE AUTHORS

L. Garimella earned his M.S. in materials science and engineering at the University of Tennessee in 1997. He is currently working at an Internet company. Mr. Garimella is a member of TMS.

P.K. Liaw earned his Ph.D. in materials science and engineering at Northwestern University in 1980. He is a professor and Ivan Racheff Chair of Excellence in the Department of Materials Science and Engineering at the University of Tennessee. Dr. Liaw is also a member of TMS.

D.L. Klarstrom earned his Ph.D. in metallurgical engineering at the University of Wisconsin–Madison. He is currently director of Haynes International. Dr. Klarstrom is also a member of TMS.

For more information, contact P.K. Liaw, University of Tennessee, Department of Materials Science and Engineering, 427 B. Dougherty Building, Knoxville, Tennessee 37996; (423) 974-6356; fax (423) 974-4115; e-mail pLiaw@utk.edu